

# Fokker-Planck equation of Schramm-Loewner evolution

M. N. Najafi\*

*Department of Physics, University of Mohaghegh Ardabili, P. O. Box 179, Ardabil, Iran*

(Received 1 January 2015; revised manuscript received 30 April 2015; published 10 August 2015)

In this paper we statistically analyze the Fokker-Planck (FP) equation of Schramm-Loewner evolution (SLE) and its variant  $SLE(\kappa, \rho_c)$ . After exploring the derivation and the properties of the Langevin equation of the tip of the SLE trace, we obtain the long- and short-time behaviors of the chordal SLE traces. We analyze the solutions of the FP and the corresponding Langevin equations and connect it to the conformal field theory (CFT) and present some exact results. We find the perturbative FP equation of the  $SLE(\kappa, \rho_c)$  traces and show that it is related to the higher-order correlation functions. Using the Langevin equation we find the long-time behaviors in this case. The CFT correspondence of this case is established and some exact results are presented.

DOI: [10.1103/PhysRevE.92.022113](https://doi.org/10.1103/PhysRevE.92.022113)

PACS number(s): 05.40.-a, 05.30.-d, 05.50.+q

## I. INTRODUCTION

Schramm-Loewner evolution (SLE) is a stochastic process which aims to classify the two-dimensional critical models by focusing on their geometrical quantities [1,2]. The idea of classification of probability measures of random curves growing in the upper half complex plane was first proposed by O. Schramm [1]. This technique has provided us with a new interpretation of the traditional conformal field theory (CFT) and Coulomb gas approaches. In CFTs the emphasis is on the algebraic properties of the critical models dictated by their conformal invariance [3]. Therefore it seems reasonable that there is a connection between this theory and SLE. This relation was found in the pioneering work of M. Bauer and D. Bernard [4] in which a relation was found between the central charge of CFT and the diffusivity parameter ( $\kappa$ ) of SLE.

Many papers have been published concerning the analytical and numerical properties of interfaces of various two-dimensional (2D) critical models described by SLE theory [1,5–7]. The statistical analysis of the various aspects of these critical curves contains valuable information of the model in hand. In the numerical studies of the lesser-known 2D critical models, the main concern is to extract the diffusivity parameter (referred to as  $\kappa$ ) of their critical interfaces to relate the underlying model to a CFT class [5,8]. Therefore the dependence of statistical observables to  $\kappa$  is of paramount importance in this area [2,9]. As an example of these statistical observables, one can mention the Fokker-Planck (FP) equation [10], left passage probability [9], crossing probability [2], etc., which are directly related to the diffusivity parameter ( $\kappa$ ) of SLE. In spite of many analysis addressing the FP equation for the SLE traces in various papers [11,12], a complete and comprehensive analysis of this subject is still missing in the literature, e.g., the actual behavior of the solutions of this equation in the whole domain of the model and a comprehensive investigation of the FP equation for the dipolar and radial SLE and  $SLE(\kappa, \rho_c)$  [13]. The question regarding *what are the statistical properties of the tip of the growing random curves in the  $SLE(\kappa)$  and  $SLE(\kappa, \rho_c)$*  is the main concern of this paper. The importance of the statistical analysis (such as FP equation) of  $SLE(\kappa, \rho_c)$  can be understood, e.g., for

the case in which the curve in its growth process *experiences* some boundary condition changes (bcc) in some point on the boundary of the domain of growth. This situation which occurs in most cases in the numerical analysis of the lesser-known models should be investigated within  $SLE(\kappa, \rho_c)$  theory. Such an analysis may help to analyze these behaviors.

In this paper we analyze the various aspects of the FP equation of SLE traces. To this end, we first show (review) how to employ the backward SLE equation and find the Langevin equation for the spatial coordinates of the tip of the SLE trace. We analyze these equations in short- and long-time limits and show that for ordinary (chordal) SLE in long times both horizontal and vertical components of the tip of the SLE trace behave as  $t^{\frac{1}{2}}$  ( $t = \text{time}$ ) as expected. To do so, we find the behaviors of SLE traces for long times in two ways: directly solving the FP equation and using the Langevin equation. We then connect the FP equation to the CFT and find some exact behaviors. For  $SLE(\kappa, \rho_c)$ , however, there is another preferred point on the real axis, causing the situation differ. To analyze this case we first find the behavior of the curves for short times perturbatively. The long-time behaviors are also investigated by analyzing the Langevin equation. We finally report some exact behaviors of this case by means of its CFT counterpart.

The paper is organized as follows: In Sec. II we present a short introduction to  $SLE(\kappa)$  and its variant  $SLE(\kappa, \rho_c)$ . The Sec. III has been devoted to the derivation of FP equations for the SLE traces. The FP equation for the  $SLE(\kappa, \rho_c)$  is derived in Sec. IV and the short- and long-time limits of this equation is derived in this section.

## II. SLE

As a well-known fact, the critical 2D models have special algebraic and geometrical properties. The algebraic properties of these models are described within the conformal field theories. However, these theories are unable to uncover the geometrical features of these models since it concerns the local fields defined in these models. According to Schramm's idea one can describe the interfaces of two-dimensional (2D) critical models via growth processes named as SLE. Thanks to this theory, however, a deep connection between their local properties and their global (geometrical) features has been discovered. This theory aims to describe the 2D critical models by focusing their interfaces. These nonintersecting *domain*

\*morteza.nattagh@gmail.com

walls are assumed to have two essential properties, conformal invariance and the domain Markov property. In the SLE theory one replaces the critical curve by a dynamical one.

We consider the model on the upper half plane, i.e.,  $H = \{z \in \mathbb{C}, \text{Im}z > 0\}$ . Let us denote the curve up to time  $t$  as  $\gamma_t$  and the hull  $K_t$  as the set of points which are located exactly on the  $\gamma_t$  trace or are disconnected from the infinity by  $\gamma_t$ . The complement of  $K_t$  is  $H_t := H \setminus K_t$  which is simply connected. According to Riemann mapping theorem [14] there is always a conformal mapping  $g_t(z)$  (in two dimensions) which maps  $H_t \rightarrow H$ . The map  $g_t(z)$  (commonly named as uniformizing map, meaning that it does uniformize the  $\gamma_t$  trace to the real axis) is the unique conformal mapping with  $g_t(z) = z + \frac{2t}{z} + O(\frac{1}{z^2})$  as  $z \rightarrow \infty$  known as hydrodynamical normalization. Loewner showed that this mapping satisfies the following equation [2,15,16]:

$$\partial_t g_t(z) = \frac{2}{g_t(z) - \zeta_t}, \tag{1}$$

with the initial condition  $g_{t=0}(z) = z$ . By  $g_t(z)$  the tip of the curve (up to time  $t$ ) is mapped to the point  $\zeta_t$  on the real axis. For fixed  $z$ ,  $g_t(z)$  is well defined up to time  $\tau_z$  for which  $g_t(z) = \zeta_t$ . The more formal definition of hull is therefore  $K_t = \{z \in H : \tau_z \leq t\}$ . For more information see Refs. [2,15–17]. For the critical models, it has been shown [1] that  $\zeta_t$  (referred to as the driving function) is a real-valued function proportional to the one-dimensional Brownian motion  $\zeta_t = \sqrt{\kappa} B_t$  in which  $\kappa$  is known as the diffusivity parameter. SLE aims to analyze these critical curves by classifying them into the one-parameter classes represented by  $\kappa$ .

There are three phases for these curves:

(i) *Dilute phase*. It is usually said that this phase consists of diffusivity parameters in the interval  $2 \leq \kappa \leq 4$  [4,18] in which the trace is non-self-intersecting and it does not hit the real axis. But the recent observation of  $\kappa < 2$  [19,20], which are in the dilute phase, extends this phase to  $0 \leq \kappa \leq 4$ . In this case the hull and the trace are identical:  $K_t = \gamma_t$ .

(ii) *Dense phase*. For  $4 < \kappa \leq 8$ , the trace touches itself and the real axis so a typical point is surely swallowed as  $t \rightarrow \infty$  and  $K_t \neq \gamma_t$ .

(iii) *Space-filling phase*. For  $\kappa > 8$  the curve is space filling.

There is a connection between the two phases: In the dense phase the frontier of  $K_t$  (the boundary of  $H_t$  minus any portions of the real axis) is a SLE curve. It has been shown [2] that this

simple curve is locally described by the diffusivity parameter  $\tilde{\kappa} = \frac{16}{\kappa}$  in the dilute phase.

The correspondence to CFT is via a simple relation between diffusivity parameter  $\kappa$  and the CFT-central charge  $c$ , i.e.,  $c = \frac{(3\kappa-8)(6-\kappa)}{2\kappa}$  [4].

**SLE( $\kappa, \rho_c$ )**

Let us now suppose that there is a preferred point on the real axis, namely at  $x^\infty$  as indicated in Fig. 1. We are going to analyze the random curve in the presence of this point. Note that the conformal invariance of the curve has been explicitly broken; however, the curve is self-similar. SLE( $\kappa, \rho_c$ ) is a variant of ordinary (chordal) SLE which analyzes such curves. We consider the upper half plane as above. In this theory the parameter  $\kappa$  is the same as above. The parameter  $\rho_c$  has to do with the boundary conditions (bc) imposed. The point  $x_\infty$  on the real axis marks the location where boundary condition changes (we name it  $x_\infty$  since this point may be considered the point at which the random curve returns as  $t \rightarrow \infty$ , see below). The exact value of  $\rho_c$  depends on the boundary change at this preferred point. In the corresponding CFT, the bcc imposed in  $x_\infty$  corresponds to putting a bcc operator with conformal weight  $h_{\rho_c} = \frac{\rho_c(\rho_c+4-\kappa)}{4\kappa}$  at that point [9,21,22].

For these curves the stochastic equation is the same as formula (1). The driving function  $\zeta_t$  acquires, however, a drift term with respect to the chordal SLE:

$$d\zeta_t = \sqrt{\kappa} dB_t + \frac{\rho_c}{\zeta_t - x_t^\infty} dt. \tag{2}$$

in which  $B_t$  is one-dimensional Brownian motion and  $x_t^\infty \equiv g_t(x_\infty)$  is the transformation of the point  $x_\infty$  under the action of  $g_t$ . This situation can be generalized to a setup with the arbitrary number of bcc's.

**Real-axis to real-axis random curves**

As an example of the above discussion, we consider the Fig. 1(b) in which the mentioned preferred point is the ending point of the curve (which does not go to the infinity, but after the exploration process returns to the real axis). For this setup, by using the conformal map  $\phi = x_\infty z / (x_\infty - z)$ , one can send the end point of the curve to the infinity. Since our model is conformal invariant, we can deduce that the function  $h_t = \phi \circ g_t \circ \phi^{-1}$  describes ordinary (chordal) SLE from which one easily concludes that  $g_t$  satisfies  $\partial_t g_t = 2 / (\{\phi'(g_t)(\phi(g_t) - \zeta_t)\})$  in which  $\phi'(z) \equiv \frac{d\phi}{dz}$ . The other criteria is to make the mapping

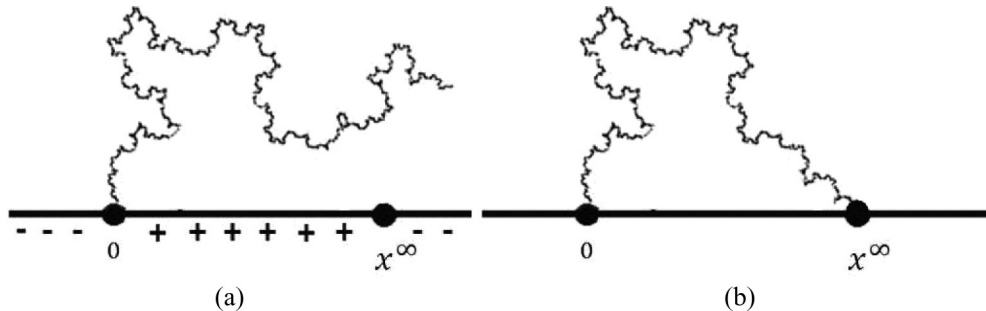


FIG. 1. (a) Schematic plot of the SLE trace in presence of a bcc point  $x^\infty$  [boundary conditions have been shown schematically by (+) and (-)]. (b) Schematic plot of the SLE trace which ends on the real axis at  $x^\infty$ .

hydrodynamically normalized. It has been shown [18] that the stochastic equation of hydrodynamically normalized  $g_t$  is the same as Eq. (1) with the price that  $\zeta_t$  acquires a drift term as follows [18]:

$$d\zeta_t = \sqrt{\kappa} dB_t + \frac{\kappa - 6}{\zeta_t - g_t(x_\infty)} dt. \quad (3)$$

In other words, this stochastic function is the driving function of the SLE( $\kappa, \rho_c$ ) with  $\rho_c = \kappa - 6$ . Thus for the critical curves from boundary to boundary, the corresponding driving function acquires a drift term. This generalization of SLE can be generalized further to have multiple preferred real axis points and multicritical curves [6]. For a review see also Refs. [2,17].

The other example is the traces which terminate surely to the real axis in the interval  $[x_0, \infty)$ . For these curves, of course the point  $x_0$  is regarded as the preferred point for which  $\rho_c = (\kappa - 6)/2$  yields dipolar SLE( $\kappa$ ) [4,6,18].

### III. DERIVATION OF FOKKER-PLANCK EQUATION

As stated above the SLE curve can be viewed as an exploration process parametrized by time  $t$ . In this section we are going to find the Langevin equation for the tip of the growing chordal SLE trace. Let us first define the shifted conformal map as follows:

$$h_t(z) \equiv g_t(z) - \zeta_t, \quad (4)$$

for which one can easily verify that

$$h_t^{-1}(w) \stackrel{d}{=} g_t^{-1}(w + \zeta_t). \quad (5)$$

In the above equation  $\stackrel{d}{=}$  means the equality of the distributions of stochastic processes. The differential equation governing  $h_t$  is

$$\partial_t h_t(z) = \frac{2}{h_t(z)} - \partial_t \zeta_t, \quad (6)$$

in which  $h_0(z) = z$ . One can retrieve the SLE trace by the relation  $\gamma(t) = \lim_{\epsilon \downarrow 0} g_t^{-1}(\zeta_t + i\epsilon) = \lim_{z \rightarrow \zeta_t} g_t^{-1}(z)$  and find the differential equation of the tip of SLE trace. The equation governing  $g_t^{-1}$  is very difficult to solve. There is a way out of this problem using the backward SLE equation. It is defined as follows (note that  $\zeta_t \stackrel{d}{=} \zeta_{-t} \stackrel{d}{=} -\zeta_t$ ) [10]:

$$\partial_t f_t(w) = -\frac{2}{f_t(w) - \zeta_t}. \quad (7)$$

It has been shown that the probability distribution of  $f_t$  is the same as  $g_t^{-1}$  [17], i.e.,

$$f_t(w) - \zeta_t \stackrel{d}{=} g_t^{-1}(w + \zeta_t) \stackrel{d}{=} h_t^{-1}(w). \quad (8)$$

The schematic representation of this equation has been sketched in Fig. 2. Therefore the tip of the SLE trace can be obtained  $\gamma_T = \lim_{w \rightarrow 0} g_T^{-1}(w + \zeta_T) = \lim_{w \rightarrow 0} h_T^{-1}(w)$ . Now we can find the trajectory of the tip of the SLE trace using the backward equation (7) for  $z_t \equiv f_t(w = 0) - \zeta_t = x_t + iy_t$  which is [notice that  $\text{Re}(\gamma_t)$  and  $\text{Im}(\gamma_t)$  have the same joint distribution as  $x_t$  and  $y_t$ ; in fact, keeping in mind that  $f_t(w = 0) - \zeta_t$  has the same distribution as the  $g_t^{-1}(\zeta_t)$  which

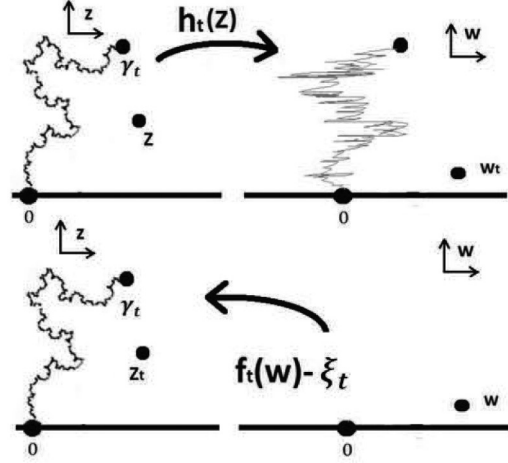


FIG. 2. Schematic representation of the conformal map  $h_t(z)$  and the backward conformal map  $f_t(w) - \zeta_t$  on the SLE trace.

is the tip of the SLE trace, we can analyze Eq. (7) instead of  $g_t^{-1}(\zeta_t)$

$$\begin{aligned} \partial_t x_t &= -\frac{2x_t}{x_t^2 + y_t^2} - \partial_t \zeta_t, \\ \partial_t y_t &= \frac{2y_t}{x_t^2 + y_t^2}, \end{aligned} \quad (9)$$

conditioned to have the initial values  $x_0 = u$  and  $y_0 = v$  in which  $w = u + iv$  is the initial point of the flow. The Fokker-Planck equation for SLE governs the probability distribution function  $\rho(x, y, t)$  for the critical curves which is the probability that the tip of the curve is at the point  $(x, y)$  on the upper half plane at time  $t$ . It is defined as  $\rho(x, y, t) = \langle \delta(x - x_t) \delta(y - y_t) \rangle$ . To obtain the FP equation, we notice that  $\rho(x, y, t + dt) - \rho(x, y, t) = \langle \delta(x - x_t - dx_t) \delta(y - y_t - dy_t) \rangle - \langle \delta(x - x_t) \delta(y - y_t) \rangle$ . Using the Langevin equations (9) of the growing SLE curve and after performing some Ito calculations, noticing that for the chordal SLE, the driving function is proportional to the Brownian motion (which implies that  $\langle (d\zeta_t)^2 \rangle = \kappa dt$ ), it can be easily proved that [10]:

$$\begin{aligned} \partial_t \rho(x, y, t) &= \left[ \frac{\kappa}{2} \partial_x^2 + \partial_x \frac{2(x - \zeta_0)}{(x - \zeta_0)^2 + y^2} \right. \\ &\quad \left. - \partial_y \frac{2y}{(x - \zeta_0)^2 + y^2} \right] \rho(x, y, t), \end{aligned} \quad (10)$$

in which  $\zeta_0$  is the point at which the curve starts to grow. The aim of this paper is to analyze the above equation.

#### A. The general properties of the FP equation

Equation (10) has the symmetry  $(x - \zeta_0) \rightarrow \lambda(x - \zeta_0)$ ,  $y \rightarrow \lambda y$ , and  $t \rightarrow \lambda^2 t$  in which  $\lambda$  is some (nonzero) positive real parameter. One can see this symmetry in another way. Let us observe the effect of the transformation  $x \rightarrow \lambda x$ ,  $y \rightarrow \lambda y$  (setting  $\zeta_0 = 0$ ) on  $\rho(x, y, t)$  which yields  $\langle \delta(\lambda x - x_t) \delta(\lambda y - y_t) \rangle = \frac{1}{\lambda^2} \langle \delta(x - \frac{1}{\lambda} x_{\lambda^2 T}) \delta(y - \frac{1}{\lambda} y_{\lambda^2 T}) \rangle$  in which  $T = \lambda^{-2} t$ . Noting that  $\frac{1}{\lambda} x_{\lambda^2 T} \stackrel{d}{=} x_T$  and  $\frac{1}{\lambda} y_{\lambda^2 T} \stackrel{d}{=} y_T$

[see Eq. (9)], we find that

$$\rho(\lambda x, \lambda y, \lambda^2 t) = \frac{1}{\lambda^2} \rho(x, y, t). \quad (11)$$

Considering also the translational symmetry of the problem, i.e.,  $x \rightarrow x + a$  and  $\zeta_0 \rightarrow \zeta_0 + a$ , we expect that  $\rho(x, y, t) = \rho(x - \zeta_0, y, t)$ . There are also two independent variables, invariant under the scale transformation, i.e.,  $\chi_t \equiv \frac{(x - \zeta_0)^2 + y^2}{t}$ ,  $\eta \equiv \frac{x - \zeta_0}{y}$  for which each invariant combination of  $x, y, t, \zeta_0$  can be expressed in terms of them. Therefore the general form of  $\rho$  has to be

$$\rho(x, y, t) = r^{-2} g(\chi_t, \eta) = t^{-1} f(\chi_t, \eta), \quad (12)$$

in which  $r \equiv \sqrt{(x - \zeta_0)^2 + y^2}$  and  $f$  and  $g$  are some functions to be determined by Eq. (10) (not to be confused with mapping  $f_t$  defined before). By setting Eq. (12) into Eq. (10) we see that it is reduced to the following form:

$$h_{\chi\chi} \partial_\chi^2 f + 2h_{\chi\eta} \partial_\chi \partial_\eta f + h_{\eta\eta} \partial_\eta^2 f + h_\chi \partial_\chi f + h_\eta \partial_\eta f + h_0 f = 0$$

$$\begin{aligned} h_{\chi\chi} &= 2\kappa \frac{\eta^2 \chi}{1 + \eta^2} \\ h_{\eta\eta} &= \frac{\kappa (1 + \eta^2)}{2\chi} \\ h_{\chi\eta} &= \kappa \eta \\ h_\chi &= \kappa + \chi + \frac{4(\eta^2 - 1)}{\eta^2 + 1} \\ h_\eta &= 4 \frac{\eta}{\chi} \\ h_0 &= 1 + \frac{4(1 - \eta^2)}{\chi(1 + \eta^2)}. \end{aligned} \quad (13)$$

It can easily be checked that this equation is a hyperbolic partial differential equation (PDE), i.e.,  $h_{\chi\eta}^2 - h_{\chi\chi} h_{\eta\eta} = 0$ . By defining  $\xi \equiv \frac{1 + \eta^2}{\chi} = \frac{t}{y^2}$  (so  $x - \zeta_0 = \eta \sqrt{\frac{t}{\xi}}$  and  $y = \sqrt{\frac{t}{\xi}}$ ) and  $f(\chi, \eta) = F(\xi, \eta)$  we obtain the canonical form:

$$\begin{aligned} \left[ \frac{1}{2} \kappa \xi \partial_\eta^2 - \left( \kappa + \frac{1 + \eta^2}{\xi} + 4 \frac{\eta^2 - 1}{\eta^2 + 1} \right) \left( \frac{\xi^2}{1 + \eta^2} \right) \partial_\xi \right. \\ \left. + \frac{4\eta\xi}{1 + \eta^2} \partial_\eta + 1 + \frac{4(1 - \eta^2)\xi}{(1 + \eta^2)^2} \right] F = 0. \end{aligned} \quad (14)$$

Before investigating further, let us explore the properties of the above equation in the limit  $y \rightarrow 0^+$  for finite  $x$  and  $t$ , i.e., large  $\eta$  and  $\xi$ . Two cases are possible in this limit, i.e.,  $x^2 \gg 4t$  (case 1 in which  $\eta^2 \gg 4\xi$ ) and  $x^2 \ll 4t$  (case 2 in which  $\eta^2 \ll 4\xi$ ). In case 1, we have:

$$\frac{1}{2} \kappa \partial_\eta^2 F - \partial_\xi F + \frac{4}{\eta} \partial_\eta F + \left( \frac{1}{\xi} \right) F = 0. \quad (15)$$

We consider the factorized form of solution, i.e.,  $F = \Pi(\eta) \Sigma(\xi)$ , from which we conclude that  $\frac{\kappa}{2\Pi} \partial_\eta^2 \Pi + \frac{4}{\eta\Pi} \partial_\eta \Pi = \frac{1}{\Sigma} \partial_\xi \Sigma - \frac{1}{\xi}$ . The right-hand side of this equation is purely a function of  $\xi$ , whereas the left-hand side is a function of  $\eta$ . Therefore both sides should be equal to a constant  $\lambda$  (in which

$\lambda$  is an arbitrary real number), so:

$$\begin{aligned} \partial_\xi \Sigma - \left( \lambda + \frac{1}{\xi} \right) \Sigma &= 0 \\ \frac{1}{2} \kappa \partial_\eta^2 \Pi + \frac{4}{\eta} \partial_\eta \Pi - \lambda \Pi &= 0 \end{aligned} \quad (16)$$

The solution of the above equations are

$$\begin{aligned} \Sigma(\xi) &= \Sigma_0 \left( \frac{\xi}{\xi_0} \right) e^{\lambda(\xi - \xi_0)} \\ \Pi(\eta) &= A_1 \eta^{-\frac{8-\kappa}{2\kappa}} I_{\frac{\kappa-8}{2\kappa}} \left( i \sqrt{\frac{2\lambda}{\kappa}} \eta \right) + A_2 \eta^{-\frac{8-\kappa}{2\kappa}} K_{\frac{\kappa-8}{2\kappa}} \left( i \sqrt{\frac{2\lambda}{\kappa}} \eta \right), \end{aligned} \quad (17)$$

in which  $I$  and  $K$  are modified Bessel functions of first and second kinds, respectively.  $\Sigma_0$  and  $\xi_0$  are constants of the first equation [so  $\Sigma_0 = \Sigma(\xi = \xi_0)$ ] and  $A_1$  and  $A_2$  are constants of the second equation. The expected behavior of these functions (being real) is satisfied only when  $\lambda = 0^-$ , which yields  $\Pi(\eta) = \eta^{-\frac{8-\kappa}{\kappa}}$ . For the determination of  $\Sigma(\xi)$ , let us observe the behavior of this function in two limits:

(1) Small  $\xi$ s, so  $|\lambda\xi|$  is a small quantity: In this limit  $\Sigma(\xi)$  is approximated by the linear relation, i.e.,  $\Sigma(\xi) \sim \xi$ , so  $\rho(x, y, t) \sim \frac{1}{y^2} \left( \frac{y}{x} \right)^{(8-\kappa)/\kappa}$ . Note that this function is independent of  $t$ . Note also that in this case we cannot speak about the limit  $y \rightarrow 0$ , since in this case (for finite  $t$ ) this leads to  $\xi \rightarrow \infty$ , which is beyond the stated limit. To investigate the properties of  $\rho(x, y, t)$  in this limit, we should take into account the other limit, i.e.,  $-\lambda\xi \gg 1$ .

(2) Sufficiently large  $\xi$ s, so  $-\lambda\xi \gg 1$ : In this limit  $\Sigma(\xi) \sim \xi e^{\lambda\xi}$  smoothly tends to zero. For the mentioned region we approximate this small function by a constant, since the tail of this  $\Sigma(\xi)$  is a smooth featureless function (although in the limit  $\xi \rightarrow \infty$  it tends to zero, the fact that this quantity can be approximated by a small constant in any interval of large  $\xi$  is sufficient for the following). Therefore we obtain that

$$\rho(x, y, t) \sim \frac{\rho_0}{t} \frac{\Sigma(\xi)}{\eta^{(8-\kappa)/\kappa}} = \frac{\rho_0}{t} \left( \frac{y}{x} \right)^{(8-\kappa)/\kappa} \Sigma(\xi), \quad (18)$$

in which  $\rho_0$  is the proportionality constant. This result reveals some important behaviors. For  $\kappa < 8$  the probability of touching the real axis boundary at fixed  $x$  value, i.e.,  $\eta = \frac{x}{y} \rightarrow \pm\infty$ , goes to zero as  $\frac{1}{\eta^{(8-\kappa)/\kappa}}$ , but for  $\kappa = 8$  there is a finite (maximum) probability of touching the boundary at a fixed  $x$  value, which is an important effect in SLE, having its root in the fact that for this case the curve is space filling. In the limit  $x^2 \ll 4t$  (case 2), however, we have

$$\left[ \frac{1}{2} \partial_\eta^2 - (\kappa + 4) \frac{\xi}{\eta^2} \partial_\xi + \frac{4}{\eta} \partial_\eta - \frac{4}{\eta^2} \right] F = 0. \quad (19)$$

We consider also the factorized form as case 1, which yields  $\frac{\kappa\eta^2}{2\Pi} \partial_\eta^2 \Pi + \frac{4\eta}{\Pi} \partial_\eta \Pi - 4 = (\kappa + 4) \frac{\xi}{\Sigma} \partial_\xi \Sigma$ . As before both sides of this equation should be equal to a constant. The resulting

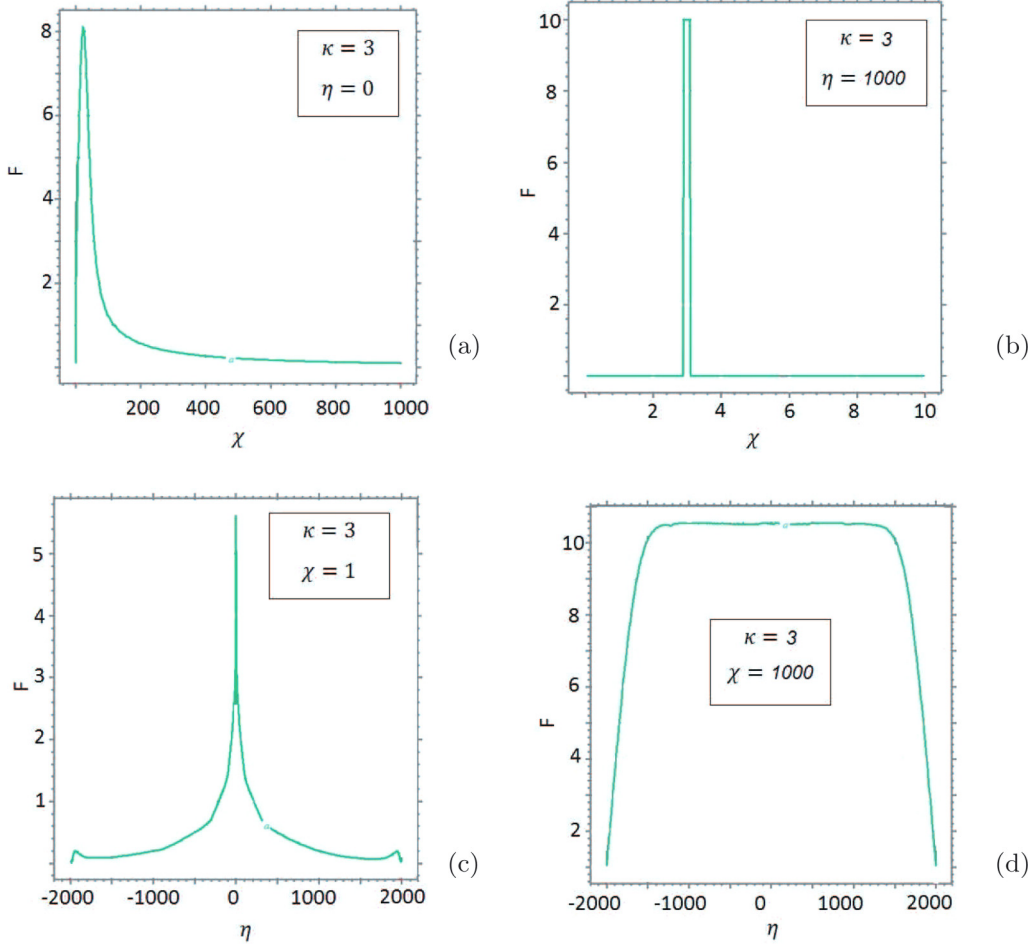


FIG. 3. (Color online) The solution of Eq. (13) for the SLE curve with diffusivity parameter  $\kappa = 3$ . In these graphs  $F$  has been plotted in terms of (a)  $\chi$  ( $\eta = 0$ ), (b)  $\chi$  ( $\eta = 1000$ ), (c)  $\eta$  ( $\chi = 1$ ), and (d)  $\eta$  ( $\chi = 1000$ ).

solutions are therefore:

$$\begin{aligned}\Sigma(\xi) &= \Sigma_0 e^{\lambda(\xi - \xi_0)} \\ \Pi(\eta) &= A_1 \eta + A_2 \eta^{-\frac{8}{\kappa}},\end{aligned}\quad (20)$$

in which  $\lambda = 0^-$  (as before) and  $A_1$  and  $A_2$  and  $\xi_0$  and  $\Sigma_0$  are some real constants as before. It is evident that  $A_1 = 0$  since one does not expect that  $F \rightarrow \infty$  for  $\eta \rightarrow \infty$ . Note also that  $\Sigma(\xi)$  goes to zero smoothly as  $\xi \rightarrow \infty$ .

Now let us discuss some aspects of the above results. Consider the case  $y \rightarrow 0^+$  for finite  $x$  and  $t$ , which corresponds to the above situations ( $\eta \rightarrow \infty$  and  $\xi \rightarrow \infty$ ). It is known that for long times  $\langle x^2 \rangle \simeq \kappa t$  (see below). Let us analyze qualitatively the properties of the FP equation in the vicinity of this point ( $y \rightarrow 0^+$  and  $x = \sqrt{\kappa t}$ ). For the case  $\kappa > 4$  one may conclude that we are approximately in case 1 [23] for which the probability that the curve passes through this point vanishes like  $F_{\kappa > 4} \sim \eta^{1 - \frac{8}{\kappa}}$ . For the case  $\kappa < 4$  (case 2 above), however, this probability vanishes like  $F_{\kappa < 4} \sim \eta^{-\frac{8}{\kappa}}$ , so  $F_{\kappa > 4} \sim \eta F_{\kappa < 4}$ . Therefore although both of these functions tend to zero at  $\eta \rightarrow \infty$ ,  $F_{\kappa < 4}$  goes to zero much faster than  $F_{\kappa > 4}$  and a change of behavior is apparent at  $\kappa = 4$ . This result has its root in the transition from the dilute phase  $\kappa < 4$  to the dense phase  $\kappa > 4$ .

To be self-contained, we have numerically solved Eq. (13). To this end we have used the finite-difference method. We have considered a lattice with dynamic mesh sizes (bounded to  $0 \leq \chi \leq 10^3$  and  $-2 \times 10^3 \leq \eta \leq 2 \times 10^3$ ). Due to the singular behavior of Eq. (13) near  $\chi = 0$  and  $\eta = 0$ , one should mesh the space near these lines more exactly (smaller) than the other points [24]. The results have been indicated in Fig. 3. As is seen in Fig. 3(a), when  $\eta = 0$  ( $x \rightarrow 0$  and  $t = \text{finite}$ ),  $F$  has a single peak at some  $\chi$ . In fact, we have observed that these peaks occur at  $\chi_0 = \frac{x_0^2 + y_0^2}{t} \simeq \frac{y_0^2}{t} = a(\kappa)$  in which  $a(\kappa) \sim (\kappa)^{-\frac{1}{2}}$ . This fact shows that for larger amounts of  $\kappa$ , at a fixed time, the vertical growth (along the  $y$  axis) of the growing curve decreases. Figure 3(b) shows this dependence for large  $\eta$ , i.e.,  $|x| \gg y$  and  $t = \text{finite}$ . The figure shows a very narrow peak appears around  $\chi_0 \simeq \frac{x_0^2}{t} = b(\kappa)$  in which  $b(\kappa) \sim \kappa$  which is expected, since for long times  $x_t \simeq \sqrt{\kappa} B_t$  [Eq. (9)]. The symmetry of  $F$  with respect to  $\eta$  is evident in Figs. 3(c) and 3(d), in which the behavior of  $F$  has been sketched in terms of  $\eta$  for the cases  $\chi = 1$  and a very large amount of  $\chi$ , respectively. For  $\chi = 1$  ( $r^2 = t$ ) it is shown that  $F$  has a peak around  $\eta = 0$  and decreases (for the positive  $\eta$  axis) as  $\eta$  increases and for  $\eta \rightarrow \infty$  (2000 in the graph) it tends to zero according to the relation obtained above. For  $\chi \gg 1$  [1000 in the Fig. 3(d)] the sensitivity of  $F$  to  $\eta$

( $= \cot \theta$  in which  $\theta \equiv \cot^{-1} \frac{x-\xi_0}{y}$ ) becomes negligible and its absolute value becomes very small.

Before closing this subsection, we notice that from the general solution of  $F(\xi, \eta)$ , we can also calculate  $\langle x^n \rangle$  and  $\langle y^n \rangle$  as follows:

$$\begin{aligned} \langle x^n \rangle(t) &= \int_{-\infty}^{\infty} dx \int_0^{\infty} dy x^n \rho(x, y, t) \\ &= \frac{1}{2} t^{\frac{n}{2}} \int_{-\infty}^{\infty} d\eta \int_0^{\infty} d\xi \frac{\eta^n F(\xi, \eta)}{\xi^{\frac{n}{2}+2}}, \end{aligned} \quad (21)$$

$$\begin{aligned} \langle y^n \rangle(t) &= \int_{-\infty}^{\infty} dx \int_0^{\infty} dy y^n \rho(x, y, t) \\ &= \frac{1}{2} t^{\frac{n}{2}} \int_{-\infty}^{\infty} d\eta \int_0^{\infty} d\xi \frac{F(\xi, \eta)}{\xi^{\frac{n}{2}+2}}, \end{aligned} \quad (22)$$

$$\begin{aligned} \langle x^n y^m \rangle(t) &= \int_{-\infty}^{\infty} dx \int_0^{\infty} dy x^n y^m \rho(x, y, t) \\ &= \frac{1}{2} t^{\frac{1}{2}(n+m)} \int_{-\infty}^{\infty} d\eta \int_0^{\infty} d\xi \frac{\eta^n F(\xi, \eta)}{\xi^{\frac{1}{2}(n+m)+2}}. \end{aligned} \quad (23)$$

We see that the  $n$ -th moment of displacement scales as  $\langle x^n \rangle \sim t^{\frac{n}{2}}$ . We can learn more about  $F$  from these relations. Since Eq. (14) is invariant under  $\eta \rightarrow -\eta$ , one can conclude that its solutions are classified into even and odd solutions with respect to the  $\eta$  component. By setting  $n = 1$  in Eq. (21), and using the fact that  $\langle x \rangle = 0$ , we can easily find that only even solutions should be taken into account, i.e.,  $F(\xi, \eta)$  is even in the  $\eta$  component. [Note that we cannot directly generalize this conclusion to the limiting case  $F \simeq \eta^{-(8-\kappa)/(\kappa)}$ . In fact, as we will see below, this function should be of the form  $(1 + \eta^2)^{-(8-\kappa)/(2\kappa)}$  which is an even function of  $\eta$  and for large amounts of  $\eta$  becomes the above result.]

In the next subsection we analyze the problem directly by means of the Langevin equations.

### B. Langevin equation for the long-time limit

In this subsection we obtain the behavior of  $\bar{x}(t) \equiv \sqrt{\langle x^2 \rangle(t)}$  and  $\langle y \rangle(t)$  for long times, using the Langevin equation [Eq. (9)]. In this limit we have  $\frac{x_t}{x_t^2 + y_t^2} \rightarrow 0$  and therefore  $dx_t \sim \sqrt{\kappa} dB_t$ . Therefore  $\bar{x}(t) \simeq \sqrt{\kappa} t^{\frac{1}{2}}$  in accordance with Eq. (21). To find the behavior of  $y_t$ , we should solve the second line of Eq. (9), with the known dependence of  $x_t$ . We approximate the right-hand side of this equation with its average, which seems to be reasonable for long times [25]. We notice that in the long-time limit, the probability distribution for  $x_t \stackrel{d}{=} \sqrt{\kappa} B_t$  is  $P(x, t) = \frac{1}{\sqrt{2\pi\kappa t}} e^{-\frac{x^2}{2\kappa t}}$ . Using the second line of Eq. (9) and replacing its right-hand side with its average, we obtain:

$$\begin{aligned} \partial_t y_t &\simeq \frac{1}{\sqrt{2\pi\kappa t}} \int_{-\infty}^{\infty} \frac{2y_t}{y_t^2 + x^2} e^{-\frac{x^2}{2\kappa t}} dx \\ \Rightarrow \partial_t y_t &\simeq \sqrt{\frac{2\pi}{\kappa t}} e^{\frac{y_t^2}{2\kappa t}} \text{Erfc}\left(\frac{y_t}{\sqrt{2\kappa t}}\right), \end{aligned} \quad (24)$$

in which  $\text{Erfc}(x) \equiv [1 - \int_0^x e^{-\eta^2} d\eta]$  is the complementary error function. To solve this equation we insert the trial function

$y_t = A\sqrt{2\kappa t} + \sqrt{2\kappa t}^{\frac{1}{2}} f_t$  into it, in which  $A$  is some constant and  $f_t$  is a function of time, to be determined. To calculate this equation we first suppose that for the long times the second term does not grow faster than the first term ( $t^{\frac{1}{2}}$ ) with time and check its validity at the end of the calculations. Therefore  $f_t$  is considered to be a small quantity for long times, so to first order of  $f_t$  we have  $e^{\frac{y_t^2}{2\kappa t}} \text{Erfc}\left(\frac{y_t}{\sqrt{2\kappa t}}\right) \simeq e^{A^2} \text{Erfc}(A) + [2Ae^{A^2} \text{Erfc}(A) - \frac{2}{\sqrt{\pi}}] f_t$ . Therefore one can easily obtain the differential equation governing  $f_t$ , i.e.,

$$\begin{aligned} t \partial_t f_t &= \frac{\sqrt{\pi}}{\kappa} \left\{ e^{A^2} \text{Erfc}(A) - \frac{\kappa}{2\sqrt{\pi}} A \right. \\ &\quad \left. + \left[ 2Ae^{A^2} \text{Erfc}(A) - \frac{2}{\sqrt{\pi}} - \frac{\kappa}{\sqrt{\pi}} \right] f_t \right\}. \end{aligned} \quad (25)$$

We choose  $A$  as the solution of  $\text{Erfc}(A) - \frac{\kappa}{2\sqrt{\pi}} A e^{-A^2} = 0$ , which can be solved by graphical methods, yielding  $A \simeq \frac{1.37}{\kappa^{0.7}}$ . After this calculation, we are able to solve the above equation and obtain:

$$y_t \simeq \frac{\gamma}{\kappa^\beta} t^{\frac{1}{2}} + f_0 t^{\alpha(\kappa)}, \quad (26)$$

in which  $\alpha(\kappa) \simeq \frac{1.88}{\kappa^{1.4}} - \frac{2}{\kappa}$ ,  $\beta \simeq 0.2$ ,  $\gamma \simeq 1.37\sqrt{2} \simeq 1.94$ , and  $f_0$  is a constant beyond this analysis. Therefore we have three cases:

$$\begin{cases} \alpha(\kappa) > \frac{1}{2} & \kappa \lesssim 0.6 \\ 0 < \alpha(\kappa) < \frac{1}{2} & 0.6 \lesssim \kappa \lesssim 0.86 \\ \alpha(\kappa) < 0 & \kappa \gtrsim 0.86 \end{cases} \quad (27)$$

The first case is beyond our analysis, since it contradicts the first assumption, i.e.,  $f_t$  should be small for long times compared with  $t^{\frac{1}{2}}$ . In the second case, i.e.,  $0.6 \lesssim \kappa \lesssim 0.86$ ,  $f_0 t^{\alpha(\kappa)}$  is a correction to the first term (it is small correction with respect to the first term for long times, since  $\alpha < 1/2$ ). For the third case, we can readily drop the correction term for long times, i.e.,  $y_t \simeq \frac{\gamma}{\kappa^\beta} t^{\frac{1}{2}}$ . For the rational CFTs in which  $2 < \kappa < 8$  the latter one is the case, and one can conclude that in the long-time limit:

$$\begin{aligned} \bar{x}_t &\simeq \sqrt{\kappa} t^{\frac{1}{2}} \\ y_t &\simeq \frac{\gamma}{\kappa^\beta} t^{\frac{1}{2}}, \end{aligned} \quad (28)$$

which is in agreement with the results of the previous subsection.

### C. CFT background

We have found the solution of the FPE of SLE growing curves in the long-time limit in the previous sections. There is another way to explore this problem within CFT techniques, which is the subject of this section.

Let us define the function  $P(x, y, \epsilon)$  as the probability that the curve passes a disk with the infinitesimal radius  $\epsilon$  centered at the point  $(x, y)$ , i.e., the probability that the distance of the point  $z = x + iy$  from the SLE curve be smaller than  $\epsilon$ . It is

defined as:

$$P(x, y, \epsilon) = \int_0^\infty \rho(x, y, t; \epsilon) dt, \quad (29)$$

in which  $\rho(x, y, t; \epsilon)$  is the probability distribution function of curves passing the distance  $\epsilon$  from the point  $(x, y)$  at the time  $t$ . Throughout this subsection we name the point at which the critical curve starts to grow as  $\zeta_0$  which is important in our analysis and in some calculations for sake of simplicity we set it to zero without loss of generality. Since  $P(x, y; \epsilon)$  is a detection probability, it has zero dimension and, consequently,  $\rho(x, y, t; \epsilon)$  is of dimension two, i.e., the behavior of these functions under the transformation  $(x - \zeta_0) \rightarrow \lambda(x - \zeta_0)$ ,  $y \rightarrow \lambda y$  is

$$\begin{aligned} P(x, y, \epsilon)|_{(x-\zeta_0) \rightarrow \lambda(x-\zeta_0), y \rightarrow \lambda y} \\ \rightarrow \int_0^\infty \rho(\lambda x, \lambda y, t; \lambda \epsilon) dt \\ = \frac{1}{\lambda^2} \int_0^\infty \rho(x, y, T; \epsilon) \times \lambda^2 dT = P(x, y, \epsilon). \end{aligned} \quad (30)$$

From general grounds it is obtained that  $P(x, y, \epsilon) \sim \epsilon^\delta P(x, y)$  [2], in which  $\delta$  is a parameter to be obtained and  $P(x, y)$  is a probability density. Now let us find the differential equation governing  $\rho(x, y, t; \epsilon)$  and  $P(x, y, \epsilon)$ . We let a SLE curve grow to time  $\delta t$  and use the conformal mapping  $g_{\delta t}$  to uniformize it. It is known from the conformal maps of the SLE that the mentioned radius  $\epsilon$  changes as  $\epsilon \rightarrow |\frac{d}{dz} g_{\delta t}(z)| \epsilon \sim \{1 - 2\delta t \text{Re}[1/(z - \zeta_0)^2]\} \epsilon$  [2] (in which  $z = x + iy$  and  $\delta t$  has been assumed to be infinitesimal, so  $\delta t^2 \simeq 0$ ). The conformal invariance of the theory dictates that after each conformal mapping  $g_{\delta t}(z)$  the measure of the SLE curves does not change, so  $\rho(x, y, t + dt; \epsilon) = \rho(x + dx, y + dy, t; \epsilon + d\epsilon)$ . To understand this, we mention that the distribution function of the system before mapping is  $\rho(x, y, \delta t, \epsilon)$ . After mapping  $g_{\delta t}(z)$ , we have a system with no hull whose distribution function is  $\rho(x + dx, y + dy, t = 0, \epsilon + d\epsilon)$ , in which  $dx = \frac{2x}{x^2 + y^2} dt$  and  $dy = -\frac{2y}{x^2 + y^2} dt$  and  $d\zeta^2 \equiv \kappa dt$  and  $\partial_{\zeta_0} = -\partial_x$ . From conformal invariance of the system we know that these distribution functions should be the same. After performing some Ito calculations and using the mapping rule of  $\epsilon$  we obtain:

$$\begin{aligned} \frac{d}{dt} \rho(x, y, t; \epsilon) = \left\{ \frac{\kappa}{2} \partial_x^2 + \frac{2(x - \zeta_0)}{(x - \zeta_0)^2 + y^2} \partial_x - \frac{2y}{(x - \zeta_0)^2 + y^2} \partial_y \right. \\ \left. - 2 \text{Re} \left[ \frac{1}{(z - \zeta_0)^2} \right] \epsilon \partial_\epsilon \right\} \rho(x, y, t; \epsilon). \end{aligned} \quad (31)$$

By integration of both sides of this equation with respect to time and using  $\epsilon \partial_\epsilon P(x, y, \epsilon) = \delta \times P(x, y, \epsilon)$ , we reach the relation:

$$\begin{aligned} \left\{ \frac{\kappa}{2} \partial_x^2 - \delta \left[ \frac{1}{(z - \zeta_0)^2} + \frac{1}{(\bar{z} - \zeta_0)^2} \right] + \frac{2(x - \zeta_0)}{(x - \zeta_0)^2 + y^2} \partial_x \right. \\ \left. - \frac{2y}{(x - \zeta_0)^2 + y^2} \partial_y \right\} P(x, y) = 0, \end{aligned} \quad (32)$$

in which as before  $z = x + iy$ . We are able also to obtain this equation using the conformal field theory. Let us analyze this problem from this point of view. Noting that the original

model has the conformal symmetry, one can easily understand that  $P(x, y)$  is proportional to the following multipoint CFT correlation function:

$$P(z, \bar{z}, \zeta_0, x^\infty) = \frac{\langle \hat{F}(x, y) \hat{F}(x, -y) \psi(\zeta_0) \psi(x^\infty) \rangle}{\langle \psi(\zeta_0) \psi(x^\infty) \rangle}. \quad (33)$$

In this equation,  $\hat{F}(x, y)$  is a *detector operator* whose value is nonzero in a field configuration only if the mentioned curve (defined in the background of other fields) passes the infinitesimal region around the point  $(x, y)$  and  $x^\infty$  is the point on the boundary at which the SLE curve ends (in other words, we have two boundary changes, one at  $\zeta_0$  and the other at  $x^\infty$ ). The operator  $\hat{F}(x, -y)$  is the image of  $\hat{F}(x, y)$  with respect to the real axis whose presence in the correlators in the boundary CFTs (BCFTs) is customary.  $\psi$  is the boundary changing operator for the CFT corresponding to underlying SLE whose conformal weight is  $h_1(\kappa) = \frac{6-\kappa}{2\kappa}$  with the second level null vector [6]:

$$\left( \frac{\kappa}{2} L_{-1}^2 - 2L_{-2} \right) \psi = 0, \quad (34)$$

in which  $L_n$ 's are the generators of the Virasoro algebra satisfying

$$[L_n, L_m] = (n - m)L_{n+m} + \frac{c}{12} n(n^2 - 1) \delta_{n+m, 0} \quad (35)$$

and  $c$  is the central charge of the underlying CFT. Using Ward identities, Eq. (34) leads to the following equation for the mentioned correlation function [3]:

$$\left( \frac{\kappa}{2} \mathcal{L}_{-1}^2 - 2\mathcal{L}_{-2} \right) \langle \hat{F}(x, y) \hat{F}(x, -y) \psi(\zeta_0) \psi(x^\infty) \rangle = 0 \quad (36)$$

with

$$\begin{aligned} \mathcal{L}_{-1} &= \frac{\partial}{\partial \zeta_0} \\ \mathcal{L}_{-2} &= \sum_i \left[ \frac{h_i}{(z_i - \zeta_0)^2} - \frac{1}{z_i - \zeta_0} \frac{\partial}{\partial z_i} \right], \end{aligned} \quad (37)$$

in which the sum is over each field in the correlation function Eq. (33) except  $\zeta_0$ . From global conformal invariance we know that

$$\begin{aligned} Q(z, \bar{z}, \zeta_0, x^\infty) &\equiv \langle \hat{F}(x, y) \hat{F}(x, -y) \psi(\zeta_0) \psi(x^\infty) \rangle \\ &= \frac{1}{(\zeta_0 - x^\infty)^{2h_1(\kappa)}} P(z, \bar{z}, \zeta_0, x^\infty) \end{aligned} \quad (38)$$

so  $Q$  satisfies the equation

$$\begin{aligned} \left\{ \frac{\kappa}{4} \partial_{\zeta_0}^2 - 2h_F \text{Re} \left[ \frac{1}{(z - \zeta_0)^2} \right] + \frac{1}{z - \zeta_0} \frac{\partial}{\partial z} + \frac{1}{\bar{z} - \zeta_0} \frac{\partial}{\partial \bar{z}} \right. \\ \left. + \frac{1}{x^\infty - \zeta_0} \frac{\partial}{\partial x^\infty} - \frac{h_1(\kappa)}{(x^\infty - \zeta_0)^2} \right\} Q = 0. \end{aligned} \quad (39)$$

In this equation  $h_F$  is the conformal weight of  $\hat{F}$ . From general grounds of CFT, we can easily find that the four-point correlation function in Eq. (33) has the following

form:

$$\begin{aligned}
P &= y^{-\frac{4}{3}h_F + \frac{2}{3}h_1(\kappa)}(x^\infty - \zeta_0)^{\frac{2}{3}h_1(\kappa) + \frac{2}{3}h_F} \\
&\quad \times [(x - x^\infty)^2 + y^2]^{\frac{1}{3}h_1(\kappa) - \frac{1}{3}h_F} \\
&\quad \times [(x - \zeta_0)^2 + y^2]^{\frac{1}{3}h_1(\kappa) - \frac{1}{3}h_F} h_0(u) \\
&= \frac{1}{y^{2h_F}} h(u), \tag{40}
\end{aligned}$$

in which  $u \equiv \text{Re}\left[\frac{(z-\zeta_0)(\bar{z}-x^\infty)}{y(x^\infty-\zeta_0)}\right]$  ( $\eta = \lim_{x^\infty \rightarrow \infty} u$ ) and  $h_0$  and  $h$  are some functions to be determined. For the limit  $x^\infty \rightarrow \infty$  the above equation reduces to the following form:

$$\left\{ \frac{\kappa}{4} \partial_{\zeta_0}^2 - 2h_F \text{Re}\left[\frac{1}{(z-\zeta_0)^2}\right] + \frac{1}{z-\zeta_0} \frac{\partial}{\partial z} + \frac{1}{\bar{z}-\zeta_0} \frac{\partial}{\partial \bar{z}} \right\} Q = 0 \tag{41}$$

and  $\text{Re}[u] = \eta$  and  $P(z, \bar{z}, \zeta_0) \sim Q(z, \bar{z}, \zeta_0) = \frac{1}{y^{2h_F}} h(\eta)$ . One can easily find that this equation is compatible with Eq. (32) by the relation  $2h_F = \delta$ . By substituting Eq. (40) into Eq. (41) we obtain (setting  $\zeta_0 = 0$ ):

$$\begin{aligned}
\left[ \frac{\kappa}{2} \partial_x^2 + \frac{2x}{x^2 + y^2} \partial_x - \frac{2y}{x^2 + y^2} \partial_y + \frac{8h_F y^2}{(x^2 + y^2)^2} \right] h(u) &= 0 \\
\Rightarrow \left[ \frac{\kappa}{2} (1 + \eta^2)^2 \partial_\eta^2 + 4\eta(1 + \eta^2) \partial_\eta + 8h_F \right] h(\eta) &= 0. \tag{42}
\end{aligned}$$

As mentioned above, the conformal weight of  $P(x, y, \epsilon)$  should be zero and the  $\epsilon^\delta$  factor in the equation  $P(x, y, \epsilon) = \epsilon^\delta P(x, y)$  compensates the factor  $y^{-2h_F}$  in front of  $P$  so one finds the form  $P(x, y, \epsilon) \sim (\frac{\epsilon}{y})^{2h_F} h(\eta)$ . If we use the trial solution  $h(\eta) = (1 + \eta^2)^\gamma$  for the above differential equation, then we obtain  $h_F = \frac{1}{2} - \frac{1}{16}\kappa$  and  $\gamma = \frac{\kappa-8}{2\kappa}$ . We know that the fractal dimension of the SLE curve is  $d_f = 1 + \kappa/8$  [2], yielding  $2h_F = 2 - d_f$ . Therefore we have:

$$P(x, y, \epsilon) \sim \left(\frac{\epsilon}{y}\right)^{2-d_f} \frac{1}{(1 + \eta^2)^{\frac{8-\kappa}{2\kappa}}} = \frac{\epsilon^{2-d_f}}{r^{(8-\kappa)/\kappa}} y^{\frac{1}{8\kappa}(\kappa-8)^2}. \tag{43}$$

First, observe that  $P \sim r^{-\frac{8-\kappa}{8}} (1 + \cot^2 \theta)^{-(8-\kappa)^2/16\kappa}$  (in which  $\eta = \cot \theta$ ), showing that as  $\kappa$  (and also the fractal dimension) increases,  $P$  becomes more long range. The dependence of  $P$  on  $\theta$  has been shown in Fig. 4. For the case  $\kappa \rightarrow 0$  we see that only for  $\theta = \frac{\pi}{2}$  is  $P$  nonzero, showing that the curves are straight vertical lines as expected, and its radial dependence is  $P \sim r^{-1}$ . The opposite limit is  $\kappa = 8$  whose curves are space filling which leads to the fact that the probability distribution is independent of  $r$  and  $\theta$ . We see from this figure that as  $\kappa$  increases, the graph is broadened, meaning that the tendency of the curve to go to  $x \rightarrow \mp\infty$  increases, which is compatible with the previous results. The other important result from this formula is that in the limit  $y \rightarrow 0$  and  $x = \text{finite}$ ,  $P = 0$  except for the case  $\kappa = 8$ . Note that this solution is compatible with the one obtained in Sec. III in which it was shown that for  $\eta \gg \xi \gg 1$ ,  $\Pi(\eta) \sim \eta^{-(8-\kappa)/\kappa}$ , which is exactly compatible with the dependence of  $P(x, y)$  on  $\eta$  obtained above, i.e.,  $(1 + \eta^2)^{-(8-\kappa)/2\kappa} \simeq \eta^{-(8-\kappa)/\kappa}$ .

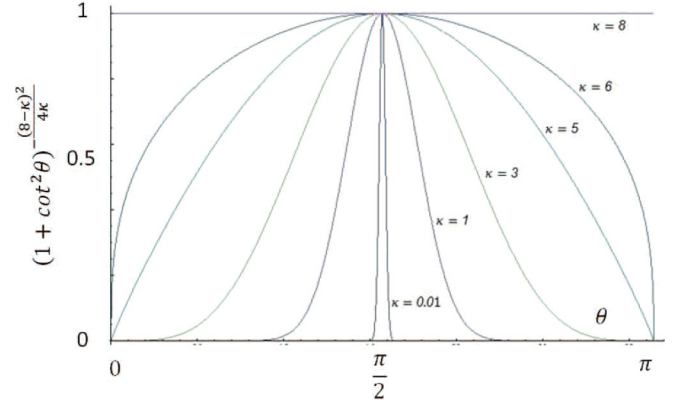


FIG. 4. (Color online) The dependence of  $P(r, \theta)$  on the angular coordinate  $\theta$  for various rates of  $\kappa$ .

#### IV. FOKKER-PLANCK EQUATION OF SLE( $\kappa, \rho_c$ )

Now we consider the SLE curves which experience a boundary condition change in some point on the real axis ( $x^\infty$ ). Specifically, we analyze the curves which go from the origin to a point on the real axis. As mentioned in Sec. II A, these curves are described by the framework of SLE( $\kappa, \kappa - 6$ ) in which we use the relation of the driving function Eq. (3). The Cartesian components of the tip of SLE growing curve satisfy the following Langevin relations:

$$\begin{aligned}
dx_t &= \frac{-2x_t}{x_t^2 + y_t^2} dt - d\zeta_t \\
dy_t &= \frac{2y_t}{x_t^2 + y_t^2} dt \\
d\zeta_t &= \sqrt{\kappa} dB_t + \frac{\rho_c}{\zeta_t - x_t^\infty} dt. \tag{44}
\end{aligned}$$

Using this equation and some calculations as above, one can calculate the change of the function  $\rho(x, y, t)$ . After some Ito calculations it can be proved that:

$$\begin{aligned}
\frac{\partial \rho}{\partial t} &= \left( \frac{\kappa}{2} \partial_x^2 + \partial_x \frac{2x}{x^2 + y^2} - \partial_y \frac{2y}{x^2 + y^2} \right) \rho \\
&\quad + \rho_c \partial_x \left\langle \frac{1}{(\zeta_t - x_t^\infty)} \delta(x - x_t) \delta(y - y_t) \right\rangle, \tag{45}
\end{aligned}$$

in which the second term in the right-hand side is due to the existence of the preferred point on the real axis.

##### A. Perturbative FPE of SLE( $\kappa, \rho_c$ )

To evaluate Eq. (45) we first consider the case  $x_t^\infty \gg \zeta_t$ , i.e., for short times of the evolution. In this limit  $x_t^\infty \approx x^\infty$  and  $\zeta_t \ll x^\infty$  so we can treat  $\frac{\zeta_t}{x^\infty}$  as the perturbation parameter. Expanding the second term in Eq. (45) in powers of this parameter we reach the formula:

$$\begin{aligned}
I &\equiv \left\langle \frac{1}{(\zeta_t - x_t^\infty)} \delta(x - x_t) \delta(y - y_t) \right\rangle \\
&= \sum_{n=0}^{\infty} \left\langle \frac{1}{x_t^\infty} \left( \frac{\zeta_t}{x_t^\infty} \right)^n \delta(x - x_t) \delta(y - y_t) \right\rangle. \tag{46}
\end{aligned}$$



To the first order of  $\frac{\zeta_t}{x^\infty}$  we have:

$$I \simeq - \left\langle \left[ \frac{1}{x_t^\infty} + \frac{\zeta_t}{(x_t^\infty)^2} \right] \delta(x - x_t) \delta(y - y_t) \right\rangle. \quad (47)$$

Taking  $x_t^\infty \simeq x^\infty$  and using the equation  $-\zeta_t = x_t + \int_0^t \frac{2x_s}{x_s^2 + y_s^2} ds$ , we can rewrite the above equation as:

$$\begin{aligned} I &\simeq \frac{-1}{x^\infty} \rho + \frac{1}{(x^\infty)^2} \left\langle \left( x_t + 2 \int_0^t \frac{x_s}{x_s^2 + y_s^2} ds \right) \right. \\ &\quad \left. \times \delta(x - x_t) \delta(y - y_t) \right\rangle \\ &= \frac{-1}{x^\infty} \rho + \frac{1}{(x^\infty)^2} (x\rho + 2\tilde{I}) \\ \tilde{I} &\equiv \left\langle \int_0^t \frac{x_s}{x_s^2 + y_s^2} ds \delta(x - x_t) \delta(y - y_t) \right\rangle. \end{aligned} \quad (48)$$

To proceed, we calculate  $\tilde{I}$ :

$$\begin{aligned} \tilde{I} &= \left\langle \int_0^t ds \int \frac{x'}{x'^2 + y'^2} \delta(x' - x_s) \right. \\ &\quad \left. \times \delta(y' - y_s) \delta(x - x_t) \delta(y - y_t) \right\rangle dx' dy' \\ &= \int_0^t ds \int \frac{x'}{x'^2 + y'^2} \rho_2(x, y, t; x', y', s | x^\infty) dx' dy'. \end{aligned} \quad (49)$$

In the above formula,  $\rho_2(x, y, t; x', y', s | x^\infty) = \langle \delta(x' - x_s) \delta(y' - y_s) \delta(x - x_t) \delta(y - y_t) \rangle$  is the probability density of the tip of the curve being in  $(x, y)$  at time  $t$  and in  $(x', y')$  at time  $s$  ( $s < t$ ). The result is

$$\begin{aligned} \frac{\partial \rho}{\partial t} &= \left[ \frac{\kappa}{2} \partial_x^2 + \partial_x \left( \frac{2x}{x^2 + y^2} - \frac{\rho_c}{x^\infty} \right) - \partial_y \frac{2y}{x^2 + y^2} \right] \\ &\quad \times \rho(x, y, x^\infty, t) \\ &+ \frac{\rho_c}{(x^\infty)^2} \left[ \partial_x (x\rho(x, y, x^\infty, t)) + 2 \int_0^t ds \int \frac{x'}{x'^2 + y'^2} \right. \\ &\quad \left. \times \partial_x \rho_2(x, y, t; x', y', s | x^\infty) dx' dy' \right] + O[(x^\infty)^{-3}]. \end{aligned} \quad (50)$$

The above formula can be generalized to any order of the perturbation parameter  $\frac{\zeta_t}{x^\infty}$ . The solutions of the above equation needs the information about  $\rho_2$  and higher-order probability functions which are less important than  $\rho$  for early times. For larger times one also may use the hypothesis  $\rho_2(x, y, t; x', y', s | x^\infty) \approx \rho(x, y, x^\infty, t) \rho(x', y', x^\infty, s)$ . Let us write everything up to  $O[(x^\infty)^{-1}]$ , i.e.,  $\rho(x, y, x^\infty, t) = \rho(x, y, t) + \epsilon \rho_1(x, y, t)$ , in which  $\epsilon \equiv \frac{r}{x^\infty}$  and  $\rho(x, y, t)$  is the solution of the FP equation for the chordal SLE, i.e., the solutions from the previous sections. Therefore, putting this function into Eq. (50), up to first order of  $\epsilon$ , we find that:

$$\begin{aligned} \frac{\partial \rho_1}{\partial t} &= \left\{ \frac{\kappa}{2} \partial_x^2 + \frac{(\kappa + 2)x}{x^2 + y^2} \partial_x - \frac{2y}{x^2 + y^2} \partial_y \right. \\ &\quad \left. + \frac{1}{2r^4} [(\kappa + 4)y^2 - 4x^2] \right\} \rho_1(x, y, t) - \frac{\rho_c}{r} \partial_x \rho(x, y, t). \end{aligned} \quad (51)$$

In this case we also have the global scale transformation symmetry and translational invariance, resulting in the same form for  $\rho_1$  as in Sec. III, i.e.,  $\rho_1 = t^{-1} \psi(\chi, \eta)$ , for  $\psi$  being a function to be determined. Straightforward calculations yield:

$$\begin{aligned} &(a_{\chi\chi} \partial_\chi^2 + 2a_{\chi\eta} \partial_\chi \partial_\eta + a_{\eta\eta} \partial_\eta^2 + a_\chi \partial_\chi + a_\eta \partial_\eta + a) \psi(\chi, \eta) \\ &= \frac{\rho_c}{\sqrt{1 + \eta^2}} \left( 2\eta \partial_\chi + \frac{1 + \eta^2}{\chi} \partial_\eta \right) f(\chi, \eta), \end{aligned} \quad (52)$$

in which  $f(\chi, \eta)$  has been defined in Eq. (12) and the coefficients are defined as:

$$\begin{aligned} a_{\chi\chi} &= 2\kappa \frac{\eta^2 \chi}{1 + \eta^2} \\ a_{\eta\eta} &= \frac{\kappa(1 + \eta^2)}{2\chi} \\ a_{\chi\eta} &= \kappa\eta \\ a_\chi &= \kappa + \chi + \frac{2[(\kappa + 2)\eta^2 - 2]}{\eta^2 + 1} \\ a_\eta &= (\kappa + 4) \frac{\eta}{\chi} \\ a &= 1 + \frac{\kappa + 4 - 4\eta^2}{2\chi(1 + \eta^2)}. \end{aligned} \quad (53)$$

This equation is parabolic PDE as the Eq. (13), since  $a_{\chi\eta}^2 - a_{\chi\chi} a_{\eta\eta} = 0$  and its canonical form is  $[\xi \equiv \frac{1 + \eta^2}{\chi}$  and  $F(\xi, \eta) = f(\chi, \eta)$  as the previous sections]:

$$\begin{aligned} &\frac{1}{2} \kappa \xi \partial_\eta^2 \psi - \left[ \kappa + \frac{1 + \eta^2}{\xi} + 2 \frac{(\kappa + 2)\eta^2 - 2}{\eta^2 + 1} \right] \left( \frac{\xi^2}{1 + \eta^2} \right) \partial_\xi \psi \\ &\quad + (\kappa + 4) \frac{\eta \xi}{1 + \eta^2} \partial_\eta \psi \\ &\quad + \left\{ 1 + \frac{\xi}{2(1 + \eta^2)^2} [(\kappa + 4) - 4\eta^2] \right\} \psi \\ &= \frac{\rho_c}{\sqrt{1 + \eta^2}} \left( -2\eta \frac{\xi^2}{1 + \eta^2} \partial_\xi + \xi \partial_\eta \right) F. \end{aligned} \quad (54)$$

Here we repeat the same steps as presented in Sec. III. For the case  $\eta \gg 1$ , we insert the factored form  $\psi = \Sigma_1(\xi) \Pi_1(\eta)$  and use the asymptotic form of  $F$  [which is  $\Sigma(\xi) \eta^{-\frac{8-\kappa}{\kappa}}$ ]. We find that:

$$\begin{aligned} &\frac{1}{2} \frac{1}{\Pi_1} \partial_\eta^2 \Pi_1 + \frac{\kappa + 4}{\eta \Pi_1} \partial_\eta \Pi_1 + \rho_c \left( 1 + \frac{8}{\kappa} \right) A \frac{1}{\eta^{1+8/\kappa} \Pi_1} \\ &\quad - \frac{1}{\Sigma_1} \partial_\xi \Sigma_1 + \frac{1}{\xi} = 0, \end{aligned} \quad (55)$$

in which  $A \equiv \frac{\Sigma_0}{\Sigma_1}$ . Assuming that  $A$  is constant, we find that  $A = \frac{\kappa(8-\kappa)}{\rho_c(8+\kappa)}$  and  $\Pi_1 = \eta^{1-8/\kappa}$ , yielding:

$$\begin{aligned} \rho(x, y, t, x_\infty) &= \left[ 1 + \frac{\rho_c(8 + \kappa)}{\kappa(8 - \kappa)} \frac{r}{x_\infty} \right] \Sigma(\xi) \Pi(\eta) \\ &\quad + O \left[ \left( \frac{r}{x_\infty} \right)^2 \right], \end{aligned} \quad (56)$$

which yields the correct form (chordal SLE) as  $\rho_c \rightarrow 0$ . This solution is obtained for  $r \ll x_\infty$  which is the region around

the tip of the curves grown in small times. For the other time limits, we should use another approach. In the next subsection we analyze other properties of the growing SLE( $\kappa, \rho_c$ ) traces, first, by its Langevin equations (in some limits) and, second, by means of CFT techniques.

### B. Langeving equation for long times

In this subsection we consider long times for which  $\frac{x_t}{x_t^2 + y_t^2} \rightarrow 0$ . To proceed we use the following assumption: The deviation of  $x_t^\infty$ , namely  $\delta x_t^\infty \equiv \sqrt{\langle x_t^{\infty 2} \rangle} - \langle x_t^\infty \rangle$  is proportional to the one for  $\zeta_t$ , i.e.,  $\bar{\zeta}_t \equiv \sqrt{\langle \zeta_t^2 \rangle}$ . Therefore the mean-field solution (to be used in this subsection) for  $x_t^\infty$  is  $x_t^\infty \simeq x^\infty + \gamma \bar{\zeta}_t$ , in which  $\gamma$  is the proportionality constant. For long times one expects that the constant  $x^\infty$  plays no role so  $x_t^\infty|_{\text{mean field}} = \gamma \bar{\zeta}_t$ . It is evident that  $\gamma$  should be larger than unity  $\gamma > 1$  for times  $t < t_{\text{exit}}$  which is defined as  $x_{t_{\text{exit}}}^\infty = \zeta_{t_{\text{exit}}}$  and the above proportionality (and the content of this subsection) is valid only for times  $1 \ll t \ll t_{\text{exit}}$ . In most situations ( $t_{\text{exit}}$ ) are so large that the above assumptions remain valid. This assumption ( $x_t^\infty = \gamma \bar{\zeta}_t$ ) can be understood by self-consistency of the calculations, i.e., as we see at the end of this subsection  $\bar{\zeta}_t \equiv \langle \zeta_t^2 \rangle \sim t^{1/2}$ . On the other hand, from the equation of  $x_t^\infty$  and replacing  $\zeta_t$  with  $\bar{\zeta}_t$  we can confirm the above assumption. There is another way to understand this assumption: In the language of conformal field theory, observables can be expressed in terms of the correlators of the primary fields which depend on the relative spatial coordinates of fields, e.g.,  $\zeta_t - x_t^\infty$ . To have time-independent observables (Martingales), the time dependence of these quantities should be the same which confirms again the proportionality relation. In this case Eq. (44) becomes (noting that in the long-time limit  $x_t \stackrel{d}{\simeq} \zeta_t$ , defining  $\tilde{\rho}_c \equiv \frac{\rho_c}{1-\gamma}$ )

$$\begin{aligned} dx_t &\simeq d\zeta_t \simeq -\sqrt{\kappa} dB_t - \frac{\tilde{\rho}_c}{\zeta_t} dt \\ \partial_t y_t &\simeq \int_{-\infty}^{\infty} \frac{2y_t}{x^2 + y_t^2} P_{\text{Bess}}(x, t) dx, \end{aligned} \quad (57)$$

in which, in the second line, we have replaced the right-hand side with its average. In this equation  $P_{\text{Bess}}(x, t)$  is the probability distribution of the Bessel process, i.e., the first expression of Eq. (57). In fact, the Fokker-Planck equation for this Langevin equation is readily:

$$\partial_t P_{\text{Bess}} = -\tilde{\rho}_c \partial_x \left( \frac{P_{\text{Bess}}}{x} \right) + \frac{\kappa}{2} \partial_x^2 P_{\text{Bess}}. \quad (58)$$

By changing variable  $\zeta \equiv \frac{x^2}{2\kappa t}$  and defining  $w \equiv t^{1/2} P_{\text{Bess}}$  we obtain

$$\zeta \frac{d^2}{d\zeta^2} w + \left( \frac{\kappa - 2\tilde{\rho}_c}{2\kappa} + \zeta \right) \frac{d}{d\zeta} w + \left( \frac{\tilde{\rho}_c}{2\kappa\zeta} + \frac{1}{2} \right) w = 0, \quad (59)$$

whose solution is

$$w(\zeta) = e^{-\zeta} \sqrt{\zeta} \left[ C_1 U \left( \frac{1}{2} - \frac{\tilde{\rho}_c}{\kappa}, \frac{3}{2} - \frac{\tilde{\rho}_c}{\kappa}, \zeta \right) + C_2 L_{\frac{1}{2} - \frac{\tilde{\rho}_c}{\kappa}}^{\frac{1}{2} - \frac{\tilde{\rho}_c}{\kappa}}(\zeta) \right], \quad (60)$$

in which  $U(a, b, z)$  is the confluent hypergeometric function and the second term is the Laguerre polynomial [26]. We expect that for the case  $\tilde{\rho}_c = 0$  and  $\kappa = 1$  we retrieve the normal distribution, i.e.,  $P_{\text{Bess}} \rightarrow t^{-1/2} e^{-\frac{x^2}{2t}}$ . Noting that  $U(\frac{1}{2}, \frac{3}{2}, \zeta) = \frac{1}{\sqrt{\zeta}}$  one can easily verify that  $C_2 = 0$ . Now let us calculate  $\langle x^2 \rangle$  and  $\langle \frac{2y_t}{x^2 + y_t^2} \rangle$  which are (note that  $\langle x \rangle = 0$ )

$$\begin{aligned} \langle x^2 \rangle &= 2\kappa t \frac{\int_0^\infty \zeta e^{-\zeta} U \left( \frac{1}{2} - \frac{\tilde{\rho}_c}{\kappa}, \frac{3}{2} - \frac{\tilde{\rho}_c}{\kappa}, \zeta \right) d\zeta}{\int_0^\infty e^{-\zeta} U \left( \frac{1}{2} - \frac{\tilde{\rho}_c}{\kappa}, \frac{3}{2} - \frac{\tilde{\rho}_c}{\kappa}, \zeta \right) d\zeta} \\ &= 2\kappa \left[ \frac{\Gamma(\frac{3}{2} - \frac{\tilde{\rho}_c}{\kappa})}{\Gamma(\frac{1}{2} - \frac{\tilde{\rho}_c}{\kappa})} \right] t \\ \left\langle \frac{2y_t}{x^2 + y_t^2} \right\rangle &= \frac{2\sqrt{2\kappa} \int_0^\infty \frac{2y_t}{2\kappa t \zeta + y_t^2} e^{-\zeta} U \left( \frac{1}{2} - \frac{\tilde{\rho}_c}{\kappa}, \frac{3}{2} - \frac{\tilde{\rho}_c}{\kappa}, \zeta \right) d\zeta}{\int_0^\infty e^{-\zeta} U \left( \frac{1}{2} - \frac{\tilde{\rho}_c}{\kappa}, \frac{3}{2} - \frac{\tilde{\rho}_c}{\kappa}, \zeta \right) d\zeta} \\ &= 2\sqrt{\frac{2}{\kappa}} t^{-1/2} \frac{\Gamma(\frac{1}{2} + \frac{\tilde{\rho}_c}{\kappa})}{\Gamma(\frac{1}{2} - \frac{\tilde{\rho}_c}{\kappa})} \chi_t^{2\frac{\tilde{\rho}_c}{\kappa}} e^{\chi_t^2} \Gamma \left( 1 - \frac{\tilde{\rho}_c}{\kappa}, \chi_t^2 \right), \end{aligned} \quad (61)$$

in which as before  $\chi_t \equiv \frac{y_t}{\sqrt{2\kappa t}}$ . It is notable that the above results are compatible with the results of Sec. III B, i.e., Eq. (24) in the limit  $\tilde{\rho}_c \rightarrow 0$  [in which  $\Gamma(1 - \frac{\tilde{\rho}_c}{\kappa}, \chi_t^2) \rightarrow \frac{\sqrt{\pi}}{2} \text{Erfc}(\chi_t^2)$  and  $\frac{\Gamma(\frac{3}{2} - \frac{\tilde{\rho}_c}{\kappa})}{\Gamma(\frac{1}{2} - \frac{\tilde{\rho}_c}{\kappa})} \rightarrow 1$ ]. These show that in the long-time limit we have  $\bar{x} \equiv \sqrt{\langle x^2 \rangle} \sim t^{1/2}$  as the chordal case and the presence of the preferred point only changes the proportionality constant of this dependence. To obtain the amount of  $y_t$ , we should solve the following equation ( $w \equiv \ln t$ ):

$$\frac{d\chi_t}{dw} = -\frac{1}{2}\chi_t + \frac{2}{\kappa} \frac{\Gamma(\frac{1}{2} + \frac{\tilde{\rho}_c}{\kappa})}{\Gamma(\frac{1}{2} - \frac{\tilde{\rho}_c}{\kappa})} \chi_t^{2\frac{\tilde{\rho}_c}{\kappa}} e^{\chi_t^2} \Gamma \left( 1 - \frac{\tilde{\rho}_c}{\kappa}, \chi_t^2 \right). \quad (62)$$

Finding the solution of the above equation is a formidable task. We argue instead that since for the chordal case  $\chi_t$  is sharply peaked nearly around an especial value  $\chi_0 \simeq \frac{2}{\kappa^{1.4}}$  (as obtained in Sec. III B), we only seek for the deviations of this behavior. To this end we expand it around this quantity:

$$\begin{aligned} &\frac{1}{-\frac{1}{2}\chi_t + \frac{2}{\kappa} \frac{\Gamma(\frac{1}{2} + \frac{\tilde{\rho}_c}{\kappa})}{\Gamma(\frac{1}{2} - \frac{\tilde{\rho}_c}{\kappa})} \chi_t^{2\frac{\tilde{\rho}_c}{\kappa}} e^{\chi_t^2} \Gamma \left( 1 - \frac{\tilde{\rho}_c}{\kappa}, \chi_t^2 \right)} \\ &= \alpha_0 + \alpha_1(\chi_t - \chi_0) + O[(\chi_t - \chi_0)^2]. \end{aligned} \quad (63)$$

Therefore we are able to determine this deviation as follows:

$$\chi_t = \frac{y_t}{\sqrt{2\kappa t}} \approx 1 + \frac{\alpha_0}{\alpha_1} \left[ -1 + \left( 1 + 2\frac{\alpha_1}{\alpha_0^2} \ln t \right)^{\frac{1}{2}} \right], \quad (64)$$

which shows the logarithmic deviation from the ordinary SLE solution.  $\alpha_0$  and  $\alpha_1$  in the above formula are

$$\alpha_0 = \frac{\Gamma\left(\frac{1}{2} - \frac{\tilde{\rho}_c}{\kappa}\right)}{-\frac{1}{\sqrt{2}}\kappa^{-3/4}\Gamma\left(\frac{1}{2} - \frac{\tilde{\rho}_c}{\kappa}\right) + 2\frac{\tilde{\rho}_c}{\kappa} + 1} e^{2\kappa^{-3/2}} \kappa^{-\frac{3\tilde{\rho}_c}{2\kappa} - 1} \Gamma\left(\frac{1}{2} + \frac{\tilde{\rho}_c}{\kappa}\right) \Gamma\left(\frac{1}{2} - \frac{\tilde{\rho}_c}{\kappa}, \frac{2}{\kappa^{3/2}}\right)$$

$$\alpha_1 = \frac{-4\sqrt{2} - \frac{\kappa\Gamma\left(\frac{1}{2} - \frac{\tilde{\rho}_c}{\kappa}\right)}{\sqrt{2}\Gamma\left(\frac{1}{2} + \frac{\tilde{\rho}_c}{\kappa}\right)} + 2\frac{\tilde{\rho}_c}{\kappa} + 2e^{\frac{2}{\kappa^{3/2}}} \kappa^{-\frac{3\tilde{\rho}_c + \kappa}{2\kappa}} \Gamma\left(\frac{1}{2} - \frac{\tilde{\rho}_c}{\kappa}, \frac{2}{\kappa^{3/2}}\right) \left(\frac{2}{\sqrt{\kappa}} + \tilde{\rho}_c\right) \Gamma\left(\frac{1}{2} + \frac{\tilde{\rho}_c}{\kappa}\right)}{2\kappa^{-3/4} \left[ \sqrt{2}\kappa^{-3/4} - 2\frac{\tilde{\rho}_c}{\kappa} + 2\frac{\Gamma\left(\frac{1}{2} + \frac{\tilde{\rho}_c}{\kappa}\right)}{\Gamma\left(\frac{1}{2} - \frac{\tilde{\rho}_c}{\kappa}\right)} e^{\frac{2}{\kappa^{3/2}}} \kappa^{-\frac{3\tilde{\rho}_c + 2\kappa}{2\kappa}} \Gamma\left(\frac{1}{2} - \frac{\tilde{\rho}_c}{\kappa}, \frac{2}{\kappa^{3/2}}\right) \right]^2} \Gamma\left(\frac{1}{2} - \frac{\tilde{\rho}_c}{\kappa}\right). \quad (65)$$

Therefore we see that the vertical component ( $y_t$ ) of the tip of the SLE trace shows serious deviations from the ordinary SLE results, in contrast to the horizontal component which has the same dependence (with modified proportionality constant):

$$\bar{x}_t = f\sqrt{2\kappa t}$$

$$y_t \simeq \sqrt{2\kappa} \left(1 - \frac{\alpha_0}{\alpha_1}\right) t^{\frac{1}{2}} + \frac{\alpha_0}{\alpha_1} \sqrt{2\kappa} \left[ \left(1 + 2\frac{\alpha_1}{\alpha_0^2} \ln t\right)^{\frac{1}{2}} - 1 \right] t^{\frac{1}{2}}, \quad (66)$$

in which  $f \equiv \sqrt{\frac{\Gamma\left(\frac{3}{2} - \frac{\tilde{\rho}_c}{\kappa}\right)}{\Gamma\left(\frac{1}{2} - \frac{\tilde{\rho}_c}{\kappa}\right)}}$ . To obtain  $\tilde{\rho}_c$  self-consistently, we should refer to the equation of  $x_t^\infty$  which is  $\frac{dx_t^\infty}{dt} = 2/(x_t^\infty - \zeta_t)$ . The approximate solution is  $x_t^\infty \simeq \sqrt{\frac{4\gamma}{\gamma-1}} t^{\frac{1}{2}}$ . To have a feeling of  $\tilde{\rho}_c$ , we approximate  $\zeta_t$  by  $\tilde{\zeta}_t \equiv \sqrt{\langle \zeta_t^2 \rangle}$ , from which one can easily obtain the self-consistency relation  $2\Gamma\left[\frac{1}{2} - \frac{\tilde{\rho}_c}{\kappa(1-\gamma)}\right] = \kappa\gamma(\gamma-1)\Gamma\left[\frac{3}{2} - \frac{\tilde{\rho}_c}{\kappa(1-\gamma)}\right]$ . Once the dependence of  $\gamma$  on  $\kappa$  and  $\rho$  is obtained, one can determine the other relevant quantities defined above.

### C. CFT prediction for the PDF of SLE( $\kappa, \rho_c$ ) traces

As Sec. III C, in this section we apply the CFT constraints to the correlation function which are representative of the probability density of the SLE( $\kappa, \rho_c$ ) random curves. The probability equals a five-point function in the corresponding conformal field theory:

$$P(x, y, \xi_0, x_\infty) = \lim_{x_0 \rightarrow \infty} \frac{\langle \hat{F}(x, y) \hat{F}(x, -y) \psi_\rho(x_\infty) \psi(\xi_0) \psi(x_0) \rangle}{\langle \psi_\rho(x_0) \psi(\xi_\infty) \psi(x_0) \rangle}, \quad (67)$$

in which  $\psi_\rho(x_\infty)$  is primary field corresponding to the boundary condition change in  $x_\infty$  with the conformal weight  $h_\rho$  which is related to  $\rho$  by the relation  $h_\rho = \frac{\rho(\rho+4-\kappa)}{4\kappa}$  [21], and  $\psi$  is the bcc operator at the point  $\zeta_0$  and the point  $x_0 \rightarrow \infty$  from and on which the SLE trace starts and ends, respectively. The operator  $\hat{F}$  is the same as Sec. III C. Therefore the problem reduces to the calculation of three-point and five-point functions which satisfy the boundary conditions. Let us define  $I(x, y, \xi_0, x_\infty)$  as the numerator of the right-hand side of Eq. (67). We have

$$P(x, y, \xi_0, x_\infty) = (x_\infty - \xi_0)^{h_\rho} I(x, y, \xi_0, x_\infty). \quad (68)$$

Using the null vector equation for  $\psi$  and after some calculations we obtain the following equation for  $P$ :

$$\left\{ \frac{\kappa}{2} \partial_{\xi_0}^2 - 2h_F \left[ \frac{1}{(z - \zeta_0)^2} + \frac{1}{(\bar{z} - \zeta_0)^2} \right] + \frac{2}{z - \zeta_0} \partial + \frac{2}{\bar{z} - \zeta_0} \bar{\partial} + \frac{2}{x_\infty - \zeta_0} \partial_{x_\infty} - \frac{2h_\rho}{(x_\infty - \zeta_0)^2} \right\} I = 0, \quad (69)$$

which yields:

$$\left[ \frac{\kappa}{2} \partial_{\xi_0}^2 + \frac{2x}{(x - \xi_0)^2 + y^2} \partial_x - \frac{2y}{(x - \xi_0)^2 + y^2} \partial_y + \frac{2}{x_\infty - \xi_0} \partial_{x_\infty} + \frac{\kappa h_\rho}{x_\infty - \xi_0} \partial_{\xi_0} + \frac{\frac{1}{2} h_\rho [\kappa(h_\rho + 1) - 8]}{(x_\infty - \xi_0)^2} - 4h_F \frac{x^2 - y^2}{(x^2 + y^2)^2} \right] P = 0. \quad (70)$$

Using global conformal invariance, one can fix  $f$  up to a function of crossing ratios and prove that  $[I = \prod_{j>i} (z_i - z_j)^{-\frac{2}{3}(h_i + h_j - \frac{1}{4}h)} I_0(u_1, u_2)]$  in which  $h_i$  is the conformal weight of the operator sitting at  $z_i$  and  $h = \sum_i h_i$ ,  $I_0$  is a function to be determined by the main equation of the theory, and  $u_1$  and  $u_2$  are the crossing ratios of the five points]. After some calculations we obtain:

$$P = \frac{1}{y^{2h_F}} h(u, v), \quad (71)$$

in which  $u$  and  $v$  are two independent variables (obtained from crossing ratios)  $u \equiv \frac{z - x_\infty}{(x_\infty - \zeta_0)}$  and  $v \equiv \frac{(\bar{z} - \xi_0)}{y}$  and  $h(u, v)$  is a function of crossing ratios to be determined. We can now substitute Eq. (71) into Eq. (70) and check that  $h$  can be written in the following form:

$$(a_{uu} \partial_u^2 + a_{vv} \partial_v^2 + a_{uv} \partial_u \partial_v + a_u \partial_u + a_v \partial_v + a_0) h = 0 \quad (72)$$

in which:

$$a_{uu} = \frac{\kappa}{2} \frac{u^3(u-1)}{2i+v} \quad a_{vv} = \frac{\kappa}{2} \frac{u(2i+v)}{u-1} \quad a_{uv} = \kappa u^2$$

$$a_u = \frac{u}{2i+u} \{2 + (u-1)(u[\kappa(h_\rho + 1) - 2] + 2)\}$$

$$a_v = 2 \frac{u(2i+v)}{v(u-1)} + \kappa h_\rho u$$

$$a_0 = \frac{8h_F u}{v(u-1)(2i+v)} + \frac{h_\rho[\kappa(h_\rho + 1) - 8]u(u-1)}{2(2i+v)}. \quad (73)$$

It is explicit that  $h$  should be a real function. In the other words, if  $h$  (real or complex) is a solution of the above equation,  $h^*$  (its complex conjugate) is also a solution, which allows us to have real solutions.

**1. The case  $\rho_c = \kappa - 6$**

For this case we can use Eqs. (39) and (38) to obtain

$$\left\{ \frac{\kappa}{4} \partial_{\zeta_0}^2 - 2h_F \operatorname{Re} \left[ \frac{1}{(z - \zeta_0)^2} \right] + \frac{1}{z - \zeta_0} \frac{\partial}{\partial z} + \frac{1}{\bar{z} - \zeta_0} \frac{\partial}{\partial \bar{z}} + \frac{1}{x^\infty - \zeta_0} \left[ (6 - \kappa) \frac{\partial}{\partial \zeta_0} + 2 \frac{\partial}{\partial x^\infty} \right] \right\} P(x, y, \zeta_0, x^\infty) = 0. \tag{74}$$

After some straightforward calculations, using the fact that  $P = \frac{1}{y^{2h_F}} h(u)$  [Eq. (40)] we obtain:

$$\left[ \frac{\kappa}{2} \partial_{\zeta_0}^2 + \frac{2(x - \zeta_0)}{(x - \zeta_0)^2 + y^2} \partial_x - \frac{2y}{(x - \zeta_0)^2 + y^2} \partial_y + \frac{6 - \kappa}{x^\infty - \zeta_0} \times \partial_{\zeta_0} + \frac{2}{x^\infty - \zeta_0} \partial_{x^\infty} + 8h_F \frac{y^2}{(x^2 + y^2)^2} \right] h(u) = 0. \tag{75}$$

Rearranging the derivatives in terms of  $u = \operatorname{Re} \frac{(z - \zeta_0)(\bar{z} - x^\infty)}{y(x^\infty - \zeta_0)} = \frac{(x - \zeta_0)(x - x^\infty)}{y(x^\infty - \zeta_0)} + \frac{y}{x^\infty - \zeta_0}$ , after some algebra it is concluded that:

$$\left[ \frac{\kappa}{2} (1 + u^2)^2 \partial_u^2 + 4u(1 + u^2) \partial_u + 8h_F \right] h(u) = 0, \tag{76}$$

which is the same as Eq. (42) by replacing  $\eta \rightarrow u$ . Therefore for the case  $\operatorname{SLE}(\kappa, \rho_c = \kappa - 6)$  we have  $P(x, y, \zeta_0, x^\infty, \epsilon) = (\frac{\epsilon}{y})^{2h_F} h(u) = (\frac{\epsilon}{y})^{2-d_f} (1 + u^2)^{-(8-\kappa)/(2\kappa)}$ .

This result is expected, since due to conformal invariance of the model we can generate  $\operatorname{SLE}(\kappa, \kappa - 6)$  curves from chordal ones by the map  $z = \phi(w) = \frac{x^\infty w}{x^\infty - w}$  in which  $z$  indicates the coordinate in which the chordal SLE grows and  $w = x + iy$  the dipolar one. Therefore we expect that  $(\epsilon')$  is the transformed

radius under  $\phi$ )

$$P_{\text{dipolar}}(w, x^\infty) = P_{\text{chordal}}[\phi(w)] = \left\{ \frac{\epsilon'}{\operatorname{Im}[\phi(w)]} \right\}^{2-d_f} \times h \left\{ \eta' = \frac{\operatorname{Re}[\phi(w)]}{\operatorname{Im}[\phi(w)]} \right\}. \tag{77}$$

We can easily verify that  $\frac{\operatorname{Re}[\phi(w)]}{\operatorname{Im}[\phi(w)]} = -u$  and since  $h(u)$  is even with respect to  $u$  we find that  $P_{\text{dipolar}}(w, x^\infty) = (\frac{\epsilon''}{y})^{2-d_f} h(u)$  in which  $\epsilon'' \equiv \frac{[(x - x^\infty)^2 + y^2]}{x^{\infty 2}} \epsilon'$  is the renormalized radius.

**V. CONCLUSION**

In this paper, we analyzed the statistics of the stochastic conformal invariant curves described by  $\operatorname{SLE}(\kappa)$  and  $\operatorname{SLE}(\kappa, \rho_c)$ . For each case we analyzed the probability distribution function  $\rho(x, y, t)$  of the tip of the SLE curve by solving the Fokker-Planck equation and by using directly the Langevin equation and the CFT techniques. The form of  $\rho(x, y, t)$  for  $\operatorname{SLE}(\kappa)$  and the (perturbative) form of this function for  $\operatorname{SLE}(\kappa, \rho)$  for some limits were shown to be compatible with the different phases of SLE curves. Using the Langevin equations, we found the short-time and the long-time asymptotic forms of the  $x_t$  and  $y_t$  components of the tip of the growing curves in each case, which shows that both these components scale as  $t^{\frac{1}{2}}$  (for long times) for chordal SLE, whereas for  $\operatorname{SLE}(\kappa, \rho)$  in the long times, the  $x$  component is only renormalized, and the  $y$  component acquires a logarithmic correction with a renormalized  $\tilde{\rho}_c$ . The connection to CFTs was also established and some exact results were extracted from the SLE-CFT duality which helps in understanding the results of the other sections.

**ACKNOWLEDGMENT**

I thank the anonymous referees on this work for the helpful comments and detailed analysis.

---

[1] Oded Schramm, *Isr. J. Math.* **118**, 221 (2000).  
 [2] J. Cardy, *Ann. Phys.* **318**, 81 (2005).  
 [3] P. Di Francesco, P. Mathieu, and D. Senegal, *Conformal Field Theory* (Springer, New York, 1997).  
 [4] M. Bauer and D. Bernard, *Commun. Math. Phys.* **239**, 493–521, (2003).  
 [5] D. Bernard, G. Boffetta, A. Celani, and G. Falkovich, *Phys. Rev. Lett.* **98**, 024501 (2007).  
 [6] M. Bauer, D. Bernard, and Kalle Kytölä, *J. Stat. Phys.* **120**, 1125 (2005).  
 [7] M. N. Najafi, S. Moghimi-Araghi, and S. Rouhani, *Phys. Rev. E* **85**, 051104 (2012).  
 [8] M. N. Najafi, S. Moghimi-Araghi, and S. Rouhani, *J. Phys. A* **45**, 095001 (2012).  
 [9] M. N. Najafi, *Phys. Rev. E* **87**, 062105 (2013).  
 [10] P. Oikonomou, I. Rushkin, I. A. Gruzberg, and L. P. Kadanoff, *J. Stat. Mech.* (2008) P01019.  
 [11] F. J. Viklund and G. F. Lawler, *Acta Mathematica* **209**, 265 (2012).  
 [12] V. Beffara, *Ann. Probab.* (2008), 1421.  
 [13] It is customary to use the phrase  $\operatorname{SLE}(\kappa, \rho)$ . In this paper we use  $\operatorname{SLE}(\kappa, \rho_c)$  in order not to be confused with the probability density  $\rho(x, y, t)$  to be defined in Sec. III.  
 [14] R. Steven Bell, *The Cauchy Transform, Potential Theory, and Conformal Mapping*, Studies in Advanced Mathematics (CRC Press, Boca Raton, FL, 1992).  
 [15] K. Loewner, *Math. Ann.* **89**, 103 (1923).  
 [16] S. Smirnov, *C. R. Acad. Sci., Ser. I, Math.* **333**, 239 (2001).  
 [17] S. Rohde and O. Schramm, *Ann. Math.* **161**, 879 (2005).  
 [18] M. Bauer, D. Bernard, and K. Kytölä, *J. Stat. Phys.* **132**, 721 (2008).  
 [19] E. Daryaei, N. A. M. Araujo, K. J. Schrenk, S. Rouhani, and H. J. Herrmann, *Phys. Rev. Lett.* **109**, 218701 (2012).  
 [20] N. Posé, K. J. Schrenk, N. A. M. Araujo, and H. J. Herrmann, *Sci. Rep.* **4**, 5495 (2014).  
 [21] K. Kytola, *J. Stat. Phys.* **123**, 1169 (2006).

- [22] Another bcc operator should be put at the origin with the conformal weight  $h_o = \frac{6-\kappa}{2\kappa}$ .
- [23] Note that in this case  $\langle x^2(t) \rangle = \kappa t > 4t$ . Therefore for this case the tip of the curve is statistically at  $x^2 = \langle x^2(t) \rangle > 4t$ , which may convince one to consider the case 1, i.e., the extreme limit  $x^2 \gg 4t$  to observe qualitatively how the behaviors change.
- [24] The MATLAB PDE toolbox has been used to solve this equation.
- [25] This approximation is reliable for long times in most cases, e.g., for the case in which the stochastic variable in hand is not directly proportional to the Brownian motion (plus some drift terms).
- [26] L. C. Andrews, *Special Functions for Engineers and Applied Mathematicians* (Macmillan, New York, 1985). For complete information about this function the reader can visit <https://en.wikipedia.org/> along with the references therein.